ON ICE BLOCKAGE OF VENT TUBES IN THE WING FUEL TANKS OF THE *EPSILON* AIRCRAFT

J.M.M. Sousa
Instituto Superior Técnico, Technical University of Lisbon
Av. Rovisco Pais, 1049-001 Lisboa, Portugal

O.D.C.S. Ferreira, B.M.M. Fundanga
Laboratório de Aeronática, Academia da Força Aérea
Granja do Marquês, 2710 Sintra, Portugal

Keywords: *aircraft icing, ice blockage, vent tube*

Abstract

A preliminary analysis of the problem of ice blockage of vent tubes in the wing fuel tanks of the Epsilon aircraft has been carried out. This included wind tunnel experiments and numerical simulations of air flow and droplet trajectories. A number of scenarios has been considered and its consequences analyzed. Subsequently, recommendations for future work and a possible modification of the vent system have been made.

1 Introduction

Fuel tanks need to be vented in order to replace the volume of used fuel with air. In addition, fuel is not a totally stable product; it will contract when cooled and expand when warmed. This means that if the aircraft is topped off with cool fuel from an underground tank and the fuel caps are sealed tightly, then the fuel will warm and expand, building up pressure in the tank. Without vents there would be no way to relieve the pressure and eventually the tank or perhaps some wing rivets would fail. On the other hand, in order to avoid fuel leaking out the vent (or spill due to overfill during fuel transfer), check valves are generally installed in the vent lines.

Vent systems need to comply with a number of requirements. The expected fuel flow must be assured in all approved operating conditions, thus preventing unwanted fuel transfer, siphoning or flow stoppage if a single vent tube is plugged with snow, ice or insects. Vents and tank airspace must interconnect, even when full, such that unequal flow (or pressure) can be avoided. This also means that vents must be properly sized for rapid altitude changes and positioned in the air stream to prevent differential pressure or suction (that may lead to uneven fuel flow, siphoning, vapor lock, fuel tank/bladder collapse or fuel starvation). Furthermore, check valves should have provisions to avoid water entering and freezing, which may cause the valve to stick open or closed. Additional stipulations related to special operating conditions (e.g., acrobatics, pressure refueling and fuel jettison), crashworthiness and fire hazards are to be considered where applicable.

Presently, the Portuguese Air Force has the aircraft *Epsilon* NC 11415 in service for basic pilot training. Under certain flight conditions (namely through clouds), blockage of the vent tubes in the wing fuel tanks of the aircraft has been reported to occur [1]. Visual inspection during formation flight has indicated that the mentioned obstruction may be a consequence of ice accretion on the vent tubes located in the lower surface of the wings, as shown in Fig. 1. If unresolved, the deficiency may ultimately lead to hazardous engine failures. Hence a modification to the vent system is now being considered. The manufacturer (EADS-SOCATA) has proposed the following solutions: the use of vented filler caps; and the installation of a redundant vent line for the central fuel tank (used for inverted flight as well). However, the latter option adds

considerable complexity to the system and vented caps should be seen as secondary vents only. A simpler and perhaps more effective solution to the above-mentioned problem might possibly be achieved through a modification to the geometry of the vent pipes. Initial efforts to accomplish this objective were directed to the understanding of the aerodynamics and ice formation process in the vent tubes of the *Epsilon* aircraft.

Fig. 1. Vent tube of the wing fuel tank.

The subject of ice accretion in airfoils is thoroughly covered in the literature (see e.g. [2,3] for a review) and many of the intrinsic ideas find application to the present problem. However, very little information was found concerning a methodology for the study of ice blockage of vent tubes.

In the present study, both wind tunnel experiments and numerical simulations have been carried out. The experiments have allowed obtaining adequate boundary conditions for the numerical simulations. Subsequently, the air flow and droplet trajectories inside a vent tube were computed.

2 Wind tunnel experiments

2.1 Flow visualization

The flow around one of the L-shaped vent tubes of the *Epsilon* aircraft was visualized using upstream smoke injection in a calibration wind tunnel. An artificial smoke generator, SAFEX FOG 2001, was employed to produce fog particles smaller than 2 μm in diameter, which acted as fluid tracers. The fog was introduced upstream the tube by the use of a 1-mm tip probe SAFEX NS1. Flood light illumination (1000 W) was also used to improve contrast. Various motion pictures were recorded to illustrate the flow features around the vent tube. A video capture is shown in Fig. 2.

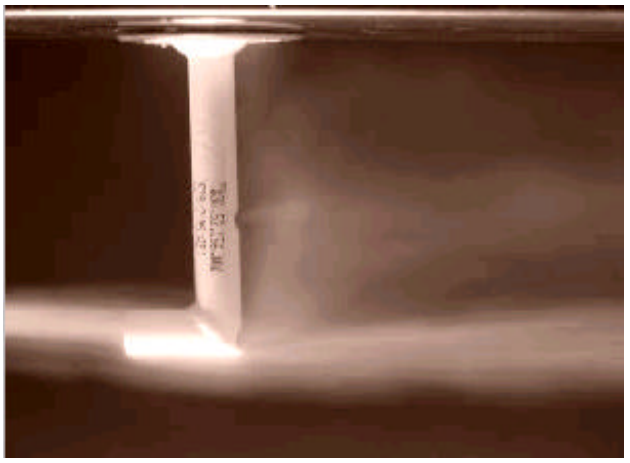

Fig. 2. Smoke flow visualization.

As expected, it was first observed that a region of separated flow establishes in the rear area of the vertical section of the vent tube. However, the high momentum jets formed in this region as a consequence of two holes in the back of the main pipe (see Fig. 2) seemed to be strong enough to penetrate the interface with the external flow.

In the left wing vent, both holes have 5 mm in diameter; in the right wing vent, the lower hole is 1 mm larger. This difference in geometry may be understood as resulting from the fact that the ventilation duct in the right wing tank is also connected with the fuel tank for inverted flight, whereas the ventilation of the left wing tank is independent. Nevertheless, in both cases, the external diameter of the vent tube is 12 mm and the internal diameter is 10 mm.

2.2 Flow measurements

Measurements of the flow velocities in the two above-referred jets were performed in a closed-

circuit wind tunnel with an open working section 1.3 m in width and 0.8 m in height. The unperturbed air speed was varied up to a maximum of 70 m/s (136 knots), closely approximating typical flight conditions for the *Epsilon* aircraft. A quantification of the pressure obtained at the top of the right wing vent tube, and theoretically inside the corresponding fuel tank, was obtained during these experiments as well.

Velocity measurements were carried out using a total pressure probe. The flow velocity at the inlet of the tube (front) was calculated from a mass balance, considering the measured velocities in the jets as mean values through the holes. These results are plotted in Fig. 3.

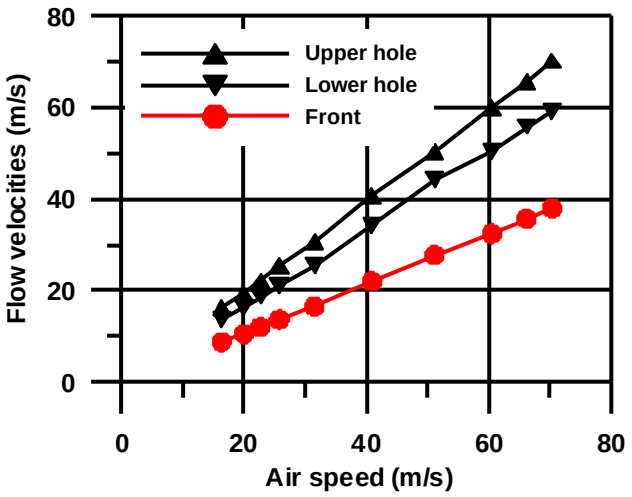

Fig. 3. Measured velocities versus air speed.

It can be seen that the jet velocities exhibit nearly a linear dependence on the air speed in the investigated range. For an air speed of about 70 m/s the mean jet velocities approach 60-70 m/s, whereas a value of 38 m/s was calculated at the vent inlet using the foregoing data. The latter value is consistent with the flow deceleration at the inlet, which in turn is associated with an increase in pressure inside the vent tube. This value has been measured relatively to the atmospheric pressure and it is shown in Fig. 4 as a function of the air speed. Not surprisingly, it can be seen that the pressure difference shows a quadratic growth with the air speed. Hence, a pressurization of the fuel tank in approximately 21 mbar might be achieved at about 70 m/s.

Globally speaking, the right wing vent tube allows a nearly constant recuperation of the total pressure in the unperturbed flow close to 70%. Subsequent measurements (not shown) have indicated that this value was slightly higher for the left wing vent tube (approximately 75%).

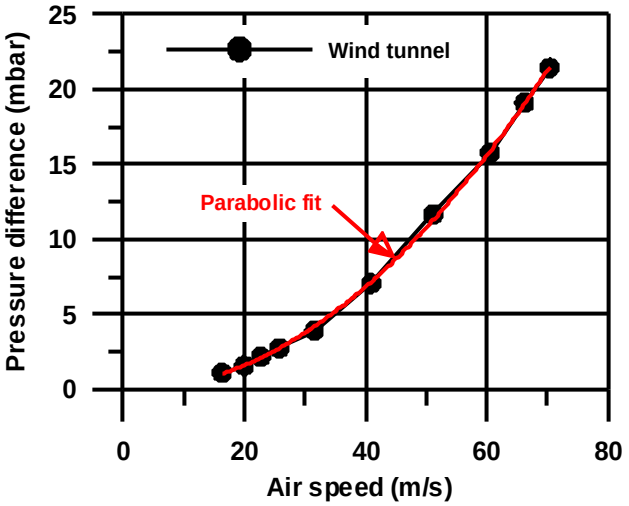

Fig. 4. Pressure difference versus air speed.

2.3 Comparison with flight tests data

Part of the wind tunnel measurements described in the previous section can, to a certain extent, be compared with available flight tests data [4]. During test flights of the *Epsilon* aircraft at 1000 ft and 10,000 ft, static pressure values were obtained from pressure transducers located in the fuel piping at the outlet of the fuel tanks. As a consequence, wind tunnel and flight tests results cannot be directly compared without a correction. The pressure at the inlet of the fuel pipes connecting with tanks will be lowered by the presence of the liquid flow. However, an approximate correction could be obtained based on the values of fuel consumption available from the flight tests as well. All sets of data, i.e. wind tunnel values, uncorrected flight values (U) and corrected flight values (C) at both heights are shown in Fig. 5 for comparison purposes.

Despite the uncertainties in the correction of the flight tests data, it seems reasonable to

conclude that fairly good agreement exists with the wind tunnel measurements. Hence, the information gathered in the latter will be used in the next section for the numerical simulations.

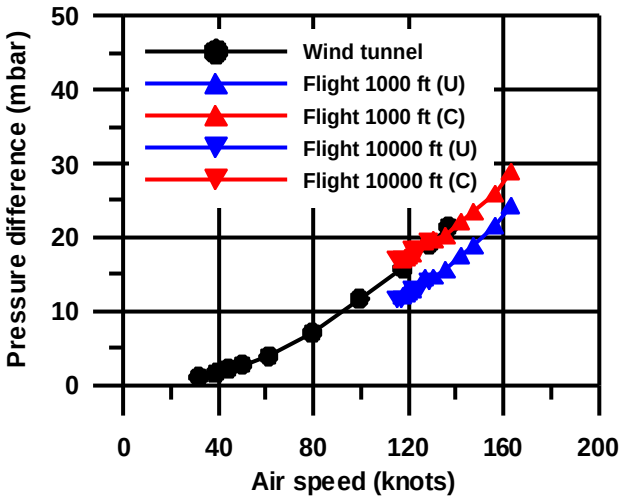

Fig. 5. Comparison: wind tunnel and flight tests.

3 Numerical simulations

3.1 Air flow inside the vent tube

The numerical simulations were based on an Eulerian-Lagrangian approach for the continuous and dispersed phase, respectively. The air flow inside the vent, i.e. the continuous phase, was computed by solving the three-dimensional, Reynolds-averaged Navier-Stokes equations. The standard *k-e* model was used for turbulence closure. In the formulation, the fluid was treated as incompressible, i.e. $r = \text{cte}$, which constitutes a reasonable assumption for a freestream Mach number of 0.21. Employing Cartesian velocity components u_i in a curvilinear frame of reference x^j, the general form of the above mentioned transport equations [5] may be given by

$$\frac{\partial}{\partial x^j}\left(r u_i b_i^j f\right) = \frac{\partial}{\partial x^j}\left(\frac{G_f}{J}\frac{\partial f}{\partial x^k} b_i^k b_i^j\right) + S_f . \qquad (1)$$

In Eq. (1) the dependent variable f is equal to one for the continuity equation, where the source term S_f is zero. The coefficients b_i^j are calculated from the coordinate transformation $x^i = x^i\left(x^j\right)$ whose Jacobian is denoted *J*. With respect to the momentum equations, the variable f stands for the velocity components u_i, the diffusion coefficient G_f is the sum of the dynamic viscosity of the fluid with the turbulent viscosity, and the source term includes additional diffusion terms as well as the pressure gradient term. See also [5] for more details on the constitution of these and the remaining transport equations. A discretization procedure based on a finite volume formulation is applied to Eq. (1), generating a set of linear equations to be solved using an appropriate iterative algorithm as described in [6].

The influence of the droplets, i.e. the dispersed phase, in the flow was ignored. This is the usual procedure in the calculation of ice accretion in airfoils [7], as the liquid water content in clouds rarely exceeds 2.0 g/m^3. For such low concentrations of the dispersed phase an uncoupled analysis is acceptable.

Calculations were made for the right wing vent tube, using the information obtained in the course of the wind tunnel experiments to setup the inlet boundary conditions. A numerical mesh containing 170,000 nodal points was employed. The outcome is displayed in Fig. 6, showing the velocity vector field and contours of the modulus of the velocity vector (absolute velocity) in a meridional cut plane. For the sake of clearness, only half of the resolution is used in the vector plot.

The mean velocities through the rear holes in the vent tube produced by the simulations were 62 m/s and 71 m/s for lower and upper holes, respectively. These values are in acceptable agreement with the experiments. Further, it can be observed that the flow is essentially characterized by the presence of three main regions of low absolute velocity. The first is established subsequently to the turn; the second corresponds to a small stagnation zone above the lower hole, associated to wall

impingement; the third is formed above the upper hole and it is a large "dead air" region. Another important feature in the flow inside the vent tube is the high-speed stream along the back wall, which is expected to promote a very effective sweep towards the exit through the upper hole.

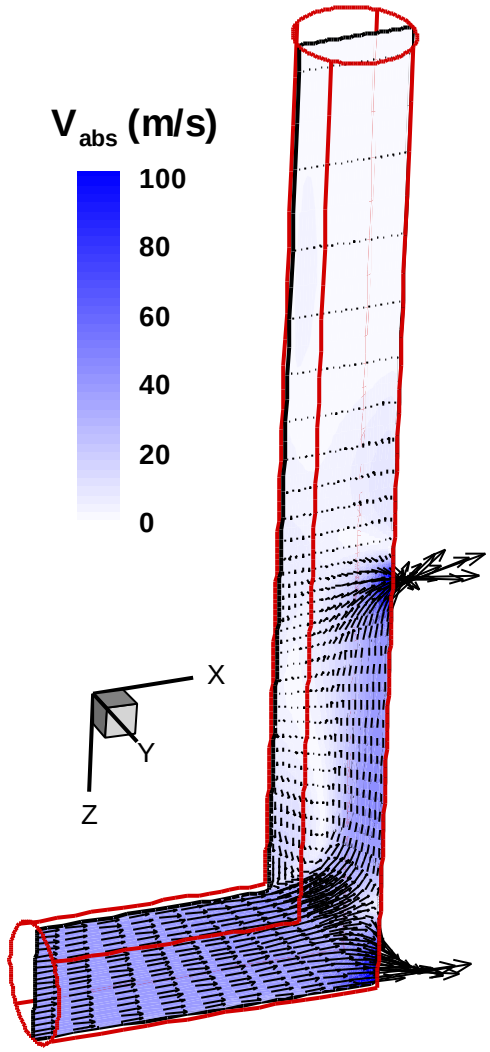

Fig. 6. Velocity field in a meridional cut plane.

The primary consequences of the flow topology observed in Fig. 6 will be discussed in the context of ice formation in the next subsection.

3.2 Droplet trajectories

Icing of the vent tubes will most certainly occur when supercooled water droplets enter the pipe and impact its inner walls. These droplets have typical diameters ranging from 10 μm to 50 μm [7], although much larger droplets may also be formed [8]. Moreover, these droplets experience relative Reynolds numbers that are low enough to ensure that they remain spherical in shape [9].

Equations of motion for the droplets may be obtained by applying Newton's Second Law to a single particle. A few simplifications to the problem can be made, namely the force due to the flow pressure gradient, the added mass force, the Basset history force, the Magnus and Saffman forces are considered negligible owing to a small gas-to-liquid density ratio r/r_d. As a result, only viscous drag and the gravity force are retained. Hence, the position vector of the droplet $\vec{x}_d$ is computed from the set of first-order ordinary differential equations

$$\frac{d\vec{x}_d}{dt} = \vec{u}_d , \qquad (2a)$$

$$\frac{d\vec{u}_d}{dt} = \frac{3}{4}\,\frac{r}{r_d}\,\frac{C_D}{d_d}\,(\vec{u}-\vec{u}_d)\,|\vec{u}-\vec{u}_d| + \vec{g} . \qquad (2b)$$

The drag coefficient C_D appearing in Eq. (2b) is taken from a standard drag correlation for solid spheres

$$C_D = \max\left[\frac{24}{Re_d}\left(1+0.15Re_d^{0.687}\right);0.44\right], \qquad (3)$$

where Re_d is the relative droplet Reynolds number given by

$$Re_d = \frac{r\,d_d\,|\vec{u}-\vec{u}_d|}{m} . \qquad (4)$$

It must be mentioned that neither droplet breakup or droplet-droplet interaction have been accounted for in this study. However, for the present problem, this is not seen as a significant shortcoming of the analysis. On the other hand, the effect of turbulence on droplet motion is only considered here indirectly. The use of a stochastic model will be required for a more complete analysis of the ice formation process

in the vent tubes. Yet, the results presented in this subsection provide already an important insight into a preliminary systematization of the phenomenon.

Droplet trajectories inside the vent tube for different droplet sizes have been computed by integrating Eqs. (2a-2b) and solving the latter expression by the "fix point" iterative method. The effect of the droplet diameter can be judged from Fig. 7, which portrays again the same meridional plane only.

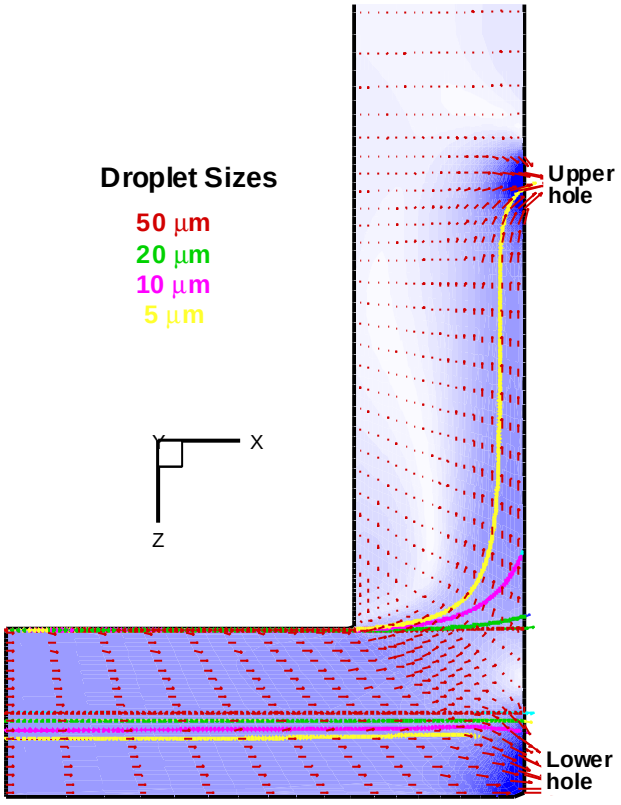

Fig. 7. Droplet trajectories for different sizes.

From the calculated trajectories one may conclude that the majority of the droplets will impact at the back wall of vent tube, as a consequence of the dominance of inertia effects. Naturally, turbulence dispersion is expected to bring a fraction of the smaller droplets to the other regions of the flow as well.

At this stage, a wide panoply of situations must be considered. The first group concerns the process of ice growth. It is known that the accreted ice can grow through either a wet or dry process [10]. Dry growth gives rise to the formation of "rime" ice, results from (nearly) immediate freezing of impacting droplets and occurs at lower temperatures (–40 ºC to –10 ºC). In contradistinction, "glaze" ice is the result of droplets coagulating in a flowing liquid film, which freezes eventually, and occurs at higher temperatures (–18 ºC to 0 ºC). The records of the flight tests at 10,000 ft indicated that the external temperature oscillated roughly between –5 ºC and 5 ºC. These data seems to substantiate the "glaze" ice scenario. However, under more critical weather conditions, temperatures as low as –15 ºC may be reached and, therefore, the formation of "rime" ice should not be ruled out.

The second group of situations regards the consequences of droplet-wall collisions. An impinging droplet will experience different fates depending on the parameters governing the process of impact. Neglecting the effect of surface roughness, the foregoing non-dimensional parameters are the Reynolds and Weber numbers defined as

$$Re = \frac{r_d \, d_d \, u_n}{m_d}, \tag{5}$$

$$We = \frac{r_d \, d_d \, u_n^2}{s_d}, \tag{6}$$

where u_n denotes a wall-normal velocity and s_d is the surface tension for a liquid-air interface.

A single non-dimensional parameter $K = \sqrt{We\sqrt{Re}}$ may be obtained from the combination of Eqs. (5)-(6) and its value may be used as an indicator for the occurrence of "deposition" or "splashing" [11], as follows

$$\begin{cases} K < 57.7 \;\Rightarrow\; \text{Deposition} \\ K \geq 57.7 \;\Rightarrow\; \text{Splashing} \end{cases}. \tag{7}$$

The simulations of droplet trajectories have shown that "splashing" (accompanied by partial "deposition") will be most likely the dominating event for the aforementioned range of particle sizes (typically K > 57.7; see also Fig. 8).

However, the larger droplets will be finely atomized upon impact, originating very small particles that follow the air flow to the exits, whereas the smaller droplets will splash into sizeable secondary ones. These secondary droplets may, according to the model described in [12] be redirected into areas of low air velocity (high residence time), adhere to the tube wall and, eventually, freeze.

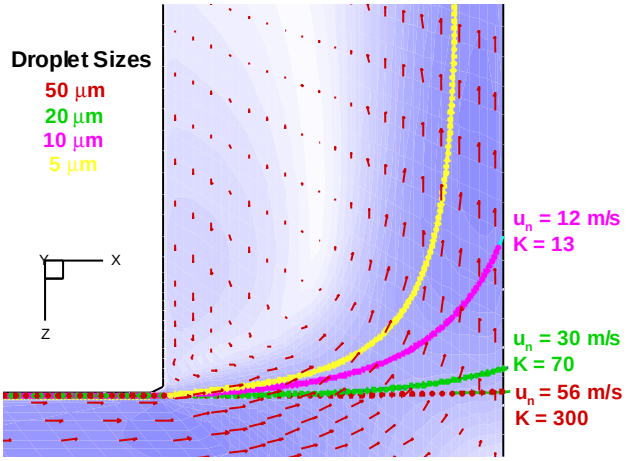

Fig. 8. Impact parameters for various droplets.

Finally, the third group of situations refers to the air flow characteristics in the impact zone. In the previous subsection, three main regions of low air velocity have been identified (Cf. Figs. 6 and 7). There, the associated low shear may preclude the droplets or the liquid film in the wall from being swept away by the air flow. Thus, ice formation will most likely commence in these areas. Based on the global topology of the flow, it seems that blockage of the vent tube will occur preferably in the massive low-speed region just above the upper hole. However, the likelihood of this scenario will also be conditioned by the circumstances discussed in the paragraphs above.

4 Future work

In order to dissipate some of the incertitude in this process, additional information regarding flight conditions under which ice blockage of the vent tubes occurs is demanded. New experiments, performed in a small icing facility, may also bring relevant insight into the analysis. On the simulations' side, stochastic modeling [13] must be incorporated on the computation of droplet trajectories, in order to be able to correctly simulate the ice accretion. Further, if the droplets remain liquid for a significant time, the complexity of the study will be much increased [14].

Although the precise implications of a modification in the geometry of the vent tubes must still be fully assessed (namely the consequences of an alteration in the pressure difference), this might constitute a simple, valid option. Such new geometry should avoid the impact of droplets in the inner walls and minimize the low-speed air flow recirculations inside. A possible candidate, complying with the foregoing limitations, is sketched in Fig. 9.

Fig. 9. Possible new geometry of the vent tubes.

5 Conclusions

The problem of ice blockage of vent tubes in the wing fuel tanks of the *Epsilon* aircraft has been analyzed. Preliminary tests have included wind tunnel experiments and numerical simulations of air flow and droplet trajectories inside the vent tube. The study has allowed establishing a number of scenarios for the occurrence of ice accretion and subsequent blockage of the pipe. Specifically, the growth of "rime" or "glaze" ice, the formation of secondary droplets by "splashing" and the stagnation of droplets or liquid film in low-shear regions of the flow have been contemplated.

It is recommended that experiments under icing conditions should be carried out, both in wind tunnel and in flight. A precise description of the mechanisms partaking in the ice blockage

of the vent tubes can only be achieved by integrating this information in the present study. The design of an alternative configuration for the vent tubes, as the one suggested here, will also benefit from these measures.

References

[1] Flight Report - 101st Squadron. Note No. 863, May 26, 1999 (in Portuguese).

[2] Thomas SK, Cassoni RP and MacArthur CD. Aircraft Anti-Icing and De-Icing Techniques and Modeling. *J. Aircraft*, Vol. 33, No. 5, pp 841-854, 1996.

[3] Gent RW, Dart NP and Cansdale JT. Aircraft Icing. *Philos. Trans. R. Soc. London*, Ser. A 358, No. 1776, pp 2873-2911, 2000.

[4] Rodrigues A and Cabral T. Characterization of the Fuel System in the Epsilon Aircraft – Instrumentation of an Aircraft for Flight Testing. Preliminary Rept. No. 380/DMA/00, Direc. de Mecânica Aeronáutica, 2001 (in Portuguese).

[5] Peric M. A Finite Volume Method for the Prediction of Three-Dimensional Fluid Flow in Complex Ducts. Ph.D. Thesis, University of London, 1985.

[6] Coelho P and Pereira JCF. Calculation Procedure for 3-D Laminar Flows in Complex Geometries Using a Nonstaggered Nonorthogonal Grid System. *Appl. Math. Modelling*, Vol. 17, pp 562-576, 1993.

[7] Bragg MB. Predicting Rime Ice Accretion on Airfoils. *AIAA J.*, Vol. 23, No. 3, pp 381-387, 1985.

[8] Lee S and Bragg MB. Experimental Investigation of Simulated Large-Droplet Ice Shapes on Airfoil Aerodynamics. *J. Aircraft*, Vol. 36, No. 5, pp 844-850, 1999.

[9] Norment HG. Calculation of Water Drop Trajectories to and About Arbitrary Three-Dimensional Bodies in Potential Flow. NASA CR 3291, 1980.

[10] Politovich, MK. Predicting Glaze or Rime Ice Growth on Airfoils. *J. Aircraft*, Vol. 37, No. 1, pp 117-121, 2000.

[11] Mundo C, Sommerfeld M and Tropea C. Droplet-Wall Collisions: Experimental Studies of the Deformation and Breakup Process. *Int. J. Multiphase Flow*, Vol. 21, No. 2, pp 151-173, 1995.

[12] Mundo C, Tropea C and Sommerfeld M. Numerical and Experimental Investigation of Spray Characteristics in the Vicinity of a Rigid Wall. *Exp. Therm. Fluid Sci.*, Vol. 15, pp 228-237, 1997.

[13] Sommerfeld M, Kohnen G and Rüger M. Some Open Questions and Inconsistencies of Lagrangian Particle Dispersion Models. *Ninth Symposium on Turbulent Shear Flows*, Kyoto, Japan, Vol. 2, paper 15-1, 1993.

[14] Myers TG, Charpin JPF and Thompson CP. Slowly Accreting Ice Due to Supercooled Water Impacting on a Cold Surface. *Phys. Fluids*, Vol. 14, No. 1, pp 240-256, 2002.